Published online 28 November 2016

Nucleic Acids Research, 2017, Vol. 45, No. 6 ***3407–3421***
doi: 10.1093/nar/gkw1021

Genetic selection for mistranslation rescues a defective co-chaperone in yeast

Kyle S. Hoffman[1], Matthew D. Berg[1], Brian H. Shilton[1], Christopher J. Brandl[1,*] and Patrick O'Donoghue[1,2,*]

[1]Department of Biochemistry, The University of Western Ontario, London, ON N6A 5C1, Canada and [2]Department of Chemistry, The University of Western Ontario, London, ON N6A 5B7, Canada

Received July 26, 2016; Revised October 11, 2016; Editorial Decision October 17, 2016; Accepted October 18, 2016

Downloaded from https://academic.oup.com/nar/article/45/6/3407/2572057 by guest on 21 August 2022

ABSTRACT

Despite the general requirement for translation fidelity, mistranslation can be an adaptive response. We selected spontaneous second site mutations that suppress the stress sensitivity caused by a *Saccharomyces cerevisiae tti2* allele with a Leu to Pro mutation at residue 187, identifying a single nucleotide mutation at the same position (C70U) in four $tRNA^{Pro}_{UGG}$ genes. Linkage analysis and suppression by $SUF9_{G3:U70}$ expressed from a centromeric plasmid confirmed the causative nature of the suppressor mutation. Since the mutation incorporates the G3:U70 identity element for alanyl-tRNA synthetase into $tRNA^{Pro}$, we hypothesized that suppression results from mistranslation of Pro187 in $Tti2_{L187P}$ as Ala. A strain expressing $Tti2_{L187A}$ was not stress sensitive. *In vitro*, $tRNA^{Pro}_{UGG}$ (C70U) was mis-aminoacylated with alanine by alanyl–tRNA synthetase, but was not a substrate for prolyl–tRNA synthetase. Mass spectrometry from protein expressed *in vivo* and a novel GFP reporter for mistranslation confirmed substitution of alanine for proline at a rate of ∼6%. Mistranslating cells expressing $SUF9_{G3:U70}$ induce a partial heat shock response but grow nearly identically to wild-type. Introducing the same G3:U70 mutation in *SUF2* ($tRNA^{Pro}_{AGG}$) suppressed a second *tti2* allele ($tti2_{L50P}$). We have thus identified a strategy that allows mistranslation to suppress deleterious missense Pro mutations in Tti2.

INTRODUCTION

Protein synthesis is a high fidelity process that ensures accurate production of the proteome as specified by the sequence of codons in protein coding genes. Overall error rates for translation indicate one in every ∼5000 amino acids are misincorporated (1). Faithful interpretation of the genetic code requires that aminoacyl–tRNA synthetases (aaRSs) specifically recognize and ligate their cognate tRNAs with the appropriate amino acid (2). Accurate recognition is determined by specific nucleotides in the tRNA called identity elements that allow the aaRSs to discriminate between tRNA species (3,4). Altering identity nucleotides can cause loss of amino acid charging, reduced substrate affinity or a decrease in turnover (5–8). Certain changes or modifications to identity nucleotides switch tRNA identity, causing mis-aminoacylation of a tRNA by a non-cognate aaRS (9,10). Ten of the aaRSs have editing activities that prevent the formation of mis-aminoacylated tRNA species (11). While cells also have quality control mechanisms to cope with increased rates of mistranslation and protein misfolding (12–14), defects in the editing activity of aaRSs can result in cancer and neurodegeneration (15,16) and lead to a cardiac disease phenotype in mouse models (17).

In an apparent contradiction, cells are able to tolerate large amounts of amino acid mis-incorporation with respect to the standard codon assignments (18). It is estimated that *Escherichia coli* tolerates a proteome with 10% of proteins made incorrectly by activating a compensatory heat shock response to eliminate misfolded proteins (13). Under certain conditions tRNA mis-aminoacylation and the resulting mistranslation is an adaptive response (13,19–22). Despite the loss in translational fidelity, altering tRNA identity can allow cells to survive otherwise lethal mutations. Such mutant tRNAs are known to suppress missense, frameshift and nonsense mutations (23–25).

We identified a novel missense suppressor $tRNA^{Pro}$ and elucidated a mechanism that induces yeast cells to mistranslate Pro codons. We selected suppressor mutations for a stress-sensitive Leu (CTA) to Pro (CCA) substitution at residue 187 in the *Saccharomyces cerevisiae* co-chaperone Tti2. Tti2 is involved in the folding and regulation of phosphatidylinositol 3-kinase related kinases (PIKKs) (26–29). The defective *tti2* allele results in loss of function and an inability to grow under stress conditions. We demonstrate that Pro to Ala mistranslation *in vivo* restores wild-type

*To whom correspondence should be addressed. Tel: +1 519 850 2373; Fax: +1 519 661 3175; Email: patrick.odonoghue@uwo.ca
Correspondence may also be addressed to Christopher J. Brandl. Tel: +1 519 850 2395; Fax: +1 519 661 3175; Email: cbrandl@uwo.ca

© The Author(s) 2016. Published by Oxford University Press on behalf of Nucleic Acids Research.
This is an Open Access article distributed under the terms of the Creative Commons Attribution License (http://creativecommons.org/licenses/by-nc/4.0/), which permits non-commercial re-use, distribution, and reproduction in any medium, provided the original work is properly cited. For commercial re-use, please contact journals.permissions@oup.com

like growth in the $tti2_{L187P}$-containing suppressor strains, and that yeast cells tolerate this proline to alanine misincorporation. As suppression can also be engineered with $tRNA^{Pro}_{AGG}$, we have identified a general mechanism to direct proteome-wide missense Ala mutations at all Pro codons.

MATERIALS AND METHODS

Yeast strains and growth conditions

Yeast strains were grown in Yeast Peptone media containing 2% glucose (YPD) or synthetic media supplemented with nitrogenous bases and amino acids as required. For spot plate assays, strains were grown to stationary phase, normalized to cell density, then spotted in 10-fold serial dilutions onto YPD plates or YPD plates containing 6% ethanol or 6 μM tunicamycin. Cells were grown at 30°C unless otherwise indicated. For growth curves, strains were grown to stationary phase in selective media diluted 1:100 in YPD media and grown at 30°C. Optical density measurements were taken every hour and average growth rates calculated using three biological replicates per strain.

All strains used (Supplementary Table S1) were derived from either BY4741, BY4742 or BY4743 (30). The *tti2* disruption strains CY6070 and CY6857 have been described (26). YCplac111-*DED1-*$tti2_{Q276TAA}$ and YCplac111-*DED1-*$tti2_{L50P}$ were transformed into CY6070, and YCplac33-*DED1-TTI2* was lost by plating on 5-fluoroorotic acid to generate CY6874 and CY6944, respectively. CY6070 was crossed with BY4742, giving rise to the diploid strain CY6945. Haploid spore colonies of CY6945 were genotyped to identify *MATa* and *MATα* strains CY6963 and CY6965, respectively. YCplac111-*DED1-*$tti2_{L187P}$ was transformed into CY6963 and YCplac33-*DED1-TTI2* lost by plating on 5-fluoroorotic acid to generate CY7020. YCplac111-*DED1-*$tti2_{L187A}$ was plasmid shuffled into CY6963 to give CY7369. CY7093, CY7105, CY7106 and CY7108 were selected as spontaneous suppressors of the slow growth of CY7020 and contain $tP(UGG)N1_{G3:U70}$, $tP(UGG)N2_{G3:U70}$, $SUF8_{G3:U70}$ and $SUF9_{G3:U70}$, respectively. CY7222 was obtained after mating CY7108 with CY6965 and selecting a Leu+ ethanol resistant spore colony. To generate CY7243, YCplac33-*DED1-TTI2* was transformed into CY7222 and the $tti2_{L187P}$ allele lost by repeated growth on media containing leucine. This strain was crossed to CY7093. The resulting diploid strain was sporulated and Ura+ strains CY7286 containing $SUF9_{G3:U70}$ and $tP(UGG)N1_{G3:U70}$, CY7287 containing *SUF9* and *tP(UGG)N1,* and CY7288 containing $SUF9_{G3:U70}$ and *tP(UGG)N1* were identified. CY7093 was transformed with YCplac33-*DED1-TTI2* and YCplac111-*DED1-*$TTI2_{L187P}$ lost by repeated growth on media containing leucine to generate CY7355.

Yeast strain CY7416 was purchased from GE Healthcare (31). The Sik1-RFP strain used for fluorescence microscopy was provided by Martin Duennwald and has been described (32). Yeast strains CY2423, CY7450 and CY1217 contain deletions of *rpn4, atg8* and *ire1*, respectively. Each strain is derived from a spore colony of the yeast magic marker strain in the BY4743 diploid background (33).

Plasmid constructs

SUF9 (pCB2957) and $SUF9_{G3:U70}$ (pCB2948) including 500bp of upstream sequence were amplified by PCR using primers TH4224 and TH4225 (Supplementary Table S2) and wild-type or CY7108 genomic DNA, respectively. *SUF9* alleles were cloned as a HindIII fragment into YCplac33 and YCplac111.

SUF2 was amplified by PCR using genomic DNA as template with primers UA9497 and UA9498, then ligated into YCplac33 as a BamHI/EcoRI fragment (pCB3015). To introduce the suppressor mutation into the 3'-end acceptor stem, YCplac33-*SUF2* was used as template in a PCR with primers UA9498 and UB0181. This product was cloned as a SmaI/SalI fragment into YCplac33-*SUF2* (pCB3028).

A two-step PCR was used to remove the *SUF9* intron and introduce the intron into *SUF2*. *SUF9* was amplified using primer TH4224 with UF4196 and TH4225 with UF4197. The PCR products were the template in a second round of PCR with primers TH4224 and TH4225. Primers UA9497 with UF4199 and UA9498 with UF4198 were used to amplify *SUF2* in the first step, and primers UA9497 and UA9498 in the second step. *SUF9* was cloned into YCplac33 as a HindIII fragment, *SUF2* as a BamHI/EcoRI fragment.

TTI2 (pCB2595) and $tti2_{L187P}$ (pCB2599) expressed from the *DED1* promoter and containing TAP and Flag tags (34) were cloned in the *URA3* two micron plasmid YCplac195 as NotI/SacI fragments. The $tti2_{L187P}$ allele has been described (26). $tti2_{L50P}$ was isolated in an identical screen. $tti2_{L187A}$ was created by a two-step primer extension PCR. Using primers 5693-1 with TK7291, and 5693-2 with TK7290 in the first step and primers 5693-1 and 5693-2 in the second step. This product was cloned as a NotI/SacI fragment into YCplac111 (pCB3020).

Yeast alanyl–tRNA synthetase (AlaRS) gene (*ALA1*) was amplified by PCR with primers TI5697 and TI5698. The PCR product was digested with NcoI/EcoRI and EcoRI/SacI, and triple ligated into NcoI/SacI cut $pP_{RO}EX^{TM}$ HTa (Invitrogen; pCB2975).

$eGFP_{D129P}$ (CCA) was generated by QuikChange (Agilent) using eGFP expressed from the *DED1* promoter on a *URA3* centromeric plasmid (35) as template and oligonucleotides UD2159 and UD2160. *SPT7* was subsequently cloned into this vector NotI/EcoRI from YCp88-myc^9-*SPT7* (34) giving $eGFP_{D129P}$-*SPT7* (pCB3057). Primers UF4570 and UF4571 were similarly used to create $eGFP_{D129A}$-*SPT7*.

Centromeric *URA3*-containing plasmid expressing *htt103Q* from the *GAL1* promoter (36), as well as the *URA3*-containing plasmid expressing *HSE-eGFP*, were kindly provided by Martin Duennwald.

Selection of suppressor mutations of $tti2_{L187P}$

CY7020 was grown to stationary phase in YPD medium and approximately 10^6 cells from independent cultures plated onto each of 10 YPD plates containing 6% ethanol. Colonies with restored growth were confirmed after growth under non-selective conditions. Suppressor strains where Western blotting indicated an increase in Tti2 expression or where plasmid shuffling indicated that the suppressor mu-

Downloaded from https://academic.oup.com/nar/article/45/6/3407/2572057 by guest on 21 August 2022

tation was plasmid borne were eliminated. A total of 4 out of 10 colonies were taken for further characterization.

Preparation of genomic DNA

Yeast strains were grown in 25 ml YPD medium to stationary phase, harvested, washed in 10 ml of sterile water and suspended in 5 ml of water containing 100 μl of β-mercaptoethanol. After 15 min, cells were harvested and cell pellets incubated at 37°C for 1 h in 5 ml of 1 M sorbitol, 100 mM sodium citrate (pH 5.8), 10 mM ethylenediaminetetraacetic acid (EDTA) and 1 mg of lyticase. Cells were harvested and suspended in 1.2 ml of 150 mM NaCl, 100 mM EDTA and 0.1% sodium dodecyl sulphate (SDS). A half volume of buffered phenol was added and mixed gently for 30 min before adding a half volume of chloroform. The aqueous phase was collected and the extraction repeated. Nucleic acids were precipitated with two volumes of ethanol and incubating at −20°C for 15 min. Precipitated nucleic acids were pelleted, washed with 80% ethanol and suspended in 500 μl of Tris-EDTA buffer. RNase was added to 20 μg/ml and incubated at 37°C for 1 h. Nucleic acids were purified using phenol:chloroform:isoamyl alcohol (25:24:1), followed by chloroform:isoamyl alcohol (24:1) extraction and precipitated with 2.5 volumes of 95% ethanol. Genomic DNA was washed in 75% ethanol, air dried, then resuspended in 50 μl of H_2O.

Genome sequencing and analysis

Samples were processed at the London Regional Genomics Centre (http://www.lrgc.ca) using the Illumina MiSeq (Illumina, Inc.). High molecular weight DNA was quantified using the Qubit DNA HS reagent (Life Technologies) and 1 ng from each sample processed as per the Nextera XT DNA Library Preparation Guide (Illumina, PN: 15031942 Rev. E). Briefly, samples were tagmented, amplified (via PCR with indexed primers to permit sample pooling), cleaned-up and equimolar pooled into one library. The pooled library was analyzed on an Agilent High Sensitivity DNA Bioanalyzer chip (Caliper Life Sciences) to assess size distribution. The quantity of the library was assessed via qPCR (Kapa Biosystems, Inc.). The library was sequenced on an Illumina MiSeq using 2 × 150 paired end run. Approximately 18 million reads (150 bp paired end) that mapped to the S288c genome were obtained. Data analysis was performed using CLCbio Genomics Workbench, v8.1. Paired end reads (150 bp) were mapped to the *Saccharomyces cerevisiae* S288c reference genome using the *local alignment* tool and duplicate reads removed. The *fixed ploidy variant detection* tool was used with a ploidy of one, required variant probability of 90%, a minimum coverage of 10 reads and a minimum read quality score of 20. All variants that were detected in the control strain, CY7020, were removed from the analysis of each suppressor strain using the compare sample variants tool.

Preparation of tRNAs

Oligonucleotides encoding a T7 promoter and yeast tRNA genes (SUF9-1 and SUF9-2 for $tRNA^{Pro}_{UGG}$, $SUF9_{G3:U70}$-1 and $SUF9_{G3:U70}$-2 for $tRNA^{Pro}_{UGG}$ (G3:U70), and tA(AGC)D-1 and tA(AGC)D-2 for $tRNA^{Ala}_{AGC}$) were obtained from Sigma-Aldrich. Complementary oligonucleotides for each tRNA gene were phosphorylated with polynucleotide kinase (Roche Inc) at 37°C for 1 h and hybridized in T4 DNA ligase buffer (New England Biolabs) by boiling for 5 min at 95°C then gradual cooling to room temperature over 2 h. Hybridized products were ligated into pTZ19r and verified by sequencing.

Each tRNA gene was amplified in a 50 μl PCR reaction, using primers UA9593 with UA9594 for *SUF9*, UA9595 with UA9596 for *tA(AGC)D*, and UA9597 with UA9598 for $SUF9_{G3:U70}$ (Supplementary Table S2). PCR products were gel purified then used as template for in vitro transcription. Transcription reactions were carried out in 40 mM Hepes/KOH pH 8.0, 22 mM $MgCl_2$, 5 mM dithiothreitol, 1 mM spermidine, 4 mM of each NTP, 30 nM T7 RNA polymerase and 10 μg of template DNA at 37°C for 3 h. RNA transcripts were isolated on a 12% polyacrylamide gel, extracted in 3 M sodium acetate and precipitated in an equal volume of isopropanol at −80°C. tRNAs were folded by heating to 95°C for 5 min, then gradually cooling to room temperature. $MgCl_2$ (10 mM) was added at 65°C. For 3′-end labelling, 2 μg of folded tRNA was incubated at 37°C for 1 h with CCA adding enzyme and [α-^{32}P] ATP (PerkinElmer) as described in (37). Labeled tRNAs were purified using BioSpin30 columns (Bio-Rad Laboratories, Inc.).

Protein purification

Yeast strains expressing YEplac195-TAP-Flag-$tti2_{L187P}$ (*URA3*-containing two-micron plasmid) and either *SUF9* or $SUF9_{G3:U70}$ expressed from a *LEU2* centromeric plasmid (YCplac111) were grown to stationary phase in minimal medium lacking uracil and leucine, diluted 1:1000 in YPD medium and grown to an OD_{600nm} = 2.5. Cells were harvested and protein extracted by grinding cells in liquid nitrogen. Lysate was cleared by ultracentrifugation at 110 000 × *g* for 1 h. TAP-tagged Tti2 was purified using the two-step tandem affinity purification protocol as described in (38).

Yeast strain Y258 over-expressing yeast Protein A-tagged prolyl–tRNA synthetase (ProRS) (BG1805-YHR020W, GE Healthcare) was grown for 48 h in minimal media lacking uracil and containing 3% ethanol, 3% glycerol and 0.05% glucose. Cells were diluted 1:25 into the same medium and grown for another 48 h. A total of 25 ml of cells were diluted into 500 ml of YP medium containing 2% galactose. At OD_{600nm} = 3.0, cells were harvested by centrifugation. Cell pellets were lysed by grinding in liquid nitrogen. ProRS was purified by binding to IgG resin (Sigma-Aldrich) in buffer containing 10 mM Tris-HCl pH 8.0 and 150 mM NaCl for 2 h. The resin with bound protein was washed three times with 4 ml of binding buffer and purified protein was cleaved from the resin with Protease 3C (a kind gift from Elton Zeqiraj in Dr Frank Sicheri's lab) in buffer containing 50 mM Tris-HCl (pH 7.0), 150 mM NaCl, 1 mM EDTA and 1 mM dithiothreitol. This was dialyzed into the same buffer with 40% glycerol and stored at −20°C.

E. coli expressing $pP_{RO}EX$ HTa-*ALA1* was grown to stationary phase in 2 ml of LB medium containing 25 μg/ml chloramphenicol and 100 μg/ml ampicillin. Cells

Downloaded from https://academic.oup.com/nar/article/45/6/3407/2572057 by guest on 21 August 2022

were diluted 1:1000 into 500 ml of the same LB medium and grown to an OD_{600nm} = 0.6. Isopropyl β-D-1-thiogalactopyranoside was added to 1 mM and cells induced overnight at room temperature. Harvested cells were lysed in 25 mM Hepes pH 7.5, 100 mM NaCl, 1 mM EDTA and 0.5 mg/ml lysozyme. Histidine-tagged AlaRS was purified using TALON® resin (Clontech Laboratories, Inc.) as described by the manufacturer, and eluted with 100 mM imidazole. Purified protein was dialyzed overnight into 50 mM Hepes (pH 7.5), 300 mM NaCl, 40% glycerol and stored at −20°C.

Aminoacylation assay

Aminoacylation reactions were performed, as described in (39), with 3 μM tRNA, 300 nM ^{32}P-labelled tRNA, 10 mM amino acid, 5 mM ATP (pH 7.0) and either 1 μM ProRS, 100 nM AlaRS or 500 pM AlaRS. Two microliters of each reaction was spotted onto polyethyleneimine-cellulose thin layer chromatography plates (EMD Millipore) and developed in 5% acetic acid and 100 mM ammonium acetate. TLC plates were exposed to phosphor screens and imaged using a Storm 860 Phosphorimager (GE Healthcare Life Sciences). Densitometry analysis of the image was done using ImageJ 1.49i. Enzyme activities were calculated across three technical replicates.

Fluorescence microscopy and eGFP reporter assay

Yeast strains were grown to stationary phase in selectable media, diluted 1:20 and grown for 5 h before harvesting. Cells were imaged using a Nikon eclipse Ti confocal microscope coupled with a Nikon DS-Qi1Mc camera head and using differential interface contrast (DIC), GFP and RFP filters. Exposure time and gain settings were left constant across all GFP and RFP images. Cell measurements were taken using Image J 1.50i with the following protocol. The DIC, GFP and RFP images for each field of view were merged by selecting Image→ Color → Merge Channels and assigning each image to a different channel. RFP-Sik1 was used to identify the nucleus which was circled with the *oval selection* tool for each cell. The intensity of the GFP signal was calculated using the *measure* tool. Background intensity was calculated from an open area adjacent to the cell. Integrated density values were divided by the area of the oval selection and the background integrated density values subtracted from each cell measurement. An average and median value of integrated density per unit area was calculated across 150 cells per strain. R version 3.2.0 along with *ggplot2* (40) was used to generate the box plot (R scripts can be found in Supplementary Figure S1).

For the *HSE-eGFP* reporter assay, yeast strain BY4742 containing *HSE-eGFP* and *SUF9* or *HSE-eGFP* and $SUF9_{G3:U70}$ were grown to stationary phase in medium lacking leucine and uracil, diluted 1:100 in the same medium and grown for 6 h at 30°C. BY4742 containing *HSE-eGFP* was heat shocked at 42°C for 1 h and used to determine the heat shock induced eGFP signal intensity. All cell densities were normalized by optical density at 600 nm prior to measuring fluorescence. Fluorescence was measured with a BioTek Synergy H1 microplate reader at an emission wavelength of 528 nm using Gen5 2.08 software. A BY4742 strain lacking *HSE-eGFP*, and containing either *SUF9* or $SUF9_{G3:U70}$, was used to subtract background fluorescence from each respective experimental strain. The average signal intensity was calculated across three technical and three biological replicates for each strain.

Mass spectrometry

Sample preparation was performed at the Functional Proteomics Facility (University of Western Ontario, http://www.uwo.ca/biochem/fpf/). TAP-Tti2 was tandem affinity purified from BY4742 expressing either *SUF9* or $SUF9_{G3:U70}$. Tti2 was picked from a 10% polyacrylamide gel stained with Coomassie Brilliant Blue using the Ettan™ Spot Picker robotic system. Gel pieces were destained in 50 mM ammonium bicarbonate and 50% acetonitrile, reduced in 10 mM dithiothreitol (DTT), alkylated using 55 mM iodoacetamide (IAA) and digested with trypsin (prepared in 50 mM ammonium bicarbonate, pH 8). The Waters MassPREP Station (PerkinElmer) was used for in-gel digestion. Peptides were extracted in 1% formic acid and 2% acetonitrile, then lyophilized.

Nano Liquid chromatography-coupled tandem mass spectrometry (nano LC–MS/MS) analysis of the digested protein was performed with ∼250 ng of peptides on column. The peptide mixture was separated by C18 reverse-phase chromatography on an ACQUITY MClass Peptide BEH column (length, 25 cm; inner diameter (i.d.), 75 μm; particle size, 1.7 μm, Waters Inc.) using a trapping column (ACQUITY MClass Trap, Symmetry C18, length, 2 cm; i.d., 180 μm; particle size, 5 μm, Waters Inc.) and a mobile phase gradient from 5% to 40% (v/v) ACN, 0.1% (v/v) FA in 90 min with a flow rate of 300 nl/min on an MClass UHPLC (nano) chromatography system (Waters Inc.). Peptides were ionized utilizing a nanospray Flex ion source (Thermo Fisher Scientific) into an Orbitrap Elite Velos Pro mass spectrometer (Thermo Fisher Scientific) via fused silica emitter tip. FT and IT injection waveforms were enabled, 1 microscan was acquired for all scan types. FT master scan preview was enabled, as was charge state screening; singly charged ions were rejected in DDA analysis. The mass spectrometer was calibrated internally with the m/z of 445.120024. Peptide ions were fragmented using collision induced dissociation (CID). The overall acquisition was an FT/IT/CID Top 15, DDA targeted scheme using dynamic exclusion in positive ion mode. The targeted ions were the +2 and +3 charged states of the peptide of interest, GVLLAQTLLNHTFmNETNDSK, where m is oxidized Methionine and A represents the substituted amino acid.

Data files (raw format, Thermo Scientific) were searched against the Uniprot, Yeast database (6729 sequences), with the Peaks algorithm (v.7.5, Bioinformatics Solutions Inc.) using the Spider node for homology search (single point mutation). For database search, the enzyme was set to trypsin, tolerating three missed cleavages and one non-specific cleavage end. The parent mass tolerance was set to 20 ppm, and the MS/MS fragment mass tolerance, to 0.8 Da. Cysteine carbamidomethylation was set as a fixed modification, and oxidation of methionine and deamidation of Asparagine/Glutamine were tolerated as a variable modification. Global false discovery rate was set to 1% with min-

Downloaded from https://academic.oup.com/nar/article/45/6/3407/2572057 by guest on 21 August 2022

imum 1 unique peptides required for protein identification. All acquired mass spectra are available upon request.

Western blotting

Yeast strains were grown to mid-logarithmic phase then lysed with glass beads. Western blotting was performed with anti-GFP antibodies (Sigma) kindly provided by Patrick Lajoie (University of Western Ontario) and anti-Myc antibodies (Sigma), and used as previously described (41).

RESULTS

Identifying second site suppressor mutations for *tti2$_{L187P}$*

Tti2 is an Hsp90 co-chaperone required for the folding and stability of PIKK family proteins including Tra1, Mec1, Tel1 and Tor1 (27–29). We identified *tti2$_{L187P}$* and *tti2$_{Q276TAA}$* (26), and subsequently *tti2$_{L50P}$* in random screens for alleles of *TTI2* that cause stress sensitive growth. As our goal was to identify specific functions of Tti2 and its interactions, we undertook a genetic approach selecting for second-site suppressors of the slow growth caused by the *tti2$_{L187P}$* allele. CY7020 (*tti2$_{L187P}$*) was grown to stationary phase and approximately 10^6 cells plated without mutagenesis onto each of ten YPD plates containing 6% ethanol. Spontaneous suppressor strains were colony purified then examined for expression of Tti2$_{L187P}$ by Western blotting. Strains with a near wild-type level of expression of Tti2$_{L187P}$ were further characterized. Suppression was observed in each of four independent strains, CY7093, CY7105, CY7106 and CY7108 (Figure 1A), where 2:2 segregation indicated that single mutations were responsible (not shown). Whole genome sequencing was performed to reveal potential causative mutations in each strain, comparing to the parent CY7020. Interestingly, all of the strains had a cytosine to thymine point mutation at nucleotide 100 in different tRNA$^{Pro}_{UGG}$ genes (Table 1).

The CY7108 strain containing *SUF9$_{G3:U70}$* and *tti2$_{L187P}$* was characterized in further detail. To verify that the *SUF9$_{G3:U70}$* mutation was responsible for suppression, its linkage with the suppressor phenotype was analyzed. CY7108 was mated with the *tti2*-disrupted strain CY6965, which contains *TTI2* on a *URA3* centromeric plasmid. The diploid was sporulated to allow independent assortment. The resulting spore colonies were plated on 5-FOA to eliminate the wild-type copy of *TTI2* and select for strains containing *tti2$_{L187P}$*. Each spore colony was then examined for growth on medium containing ethanol to determine if there was suppression or a stress sensitive phenotype. We sequenced the *SUF9* allele of 10 spore colonies, including four without and six with the suppressor phenotype. In each case, *SUF9$_{G3:U70}$* was linked to suppression whereas slow growth was associated with the wild-type *SUF9* allele, thus indicating that *SUF9$_{G3:U70}$* was responsible for suppression.

We then introduced *SUF9* or *SUF9$_{G3:U70}$* from a centromeric plasmid into the *tti2$_{L187P}$* strain (CY7020) to determine if the mutant allele was sufficient for suppression. The plasmid expressing *SUF9$_{G3:U70}$* suppressed slow growth of the *tti2$_{L187P}$* strain on an ethanol stress plate (Figure 1B). The *SUF9$_{G3:U70}$* allele did not suppress *tti2$_{Q276TAA}$* or *tti2$_{L50P}$* (CUC to CCC), indicating that suppression is allele specific and thus *SUF9$_{G3:U70}$* acts directly by mistranslating P187 (Figure 1C). These results suggest that the G3:U70 mutation in tRNA$^{Pro}_{UGG}$ is directly responsible for the suppression of *tti2$_{L187P}$* in each of the four sequenced suppressor strains.

Suppression is due to alanine substitution for proline during translation of *tti2$_{L187P}$*

The suppressor mutation in the tRNA$^{Pro}_{UGG}$ genes results in a G3:C70 to G3:U70 base pair change in the tRNA acceptor stem (Figure 2A). The G3:U70 pair is the major identity element for AlaRS (42,43). Introducing this base pair confers alanine accepting identity to tRNA^{Cys} and tRNA^{Phe} in *E. coli* (44). We predicted that the G3:U70 base pair in tRNA$^{Pro}_{UGG}$ (C70U) results in aminoacylation with alanine and subsequent mis-incorporation of alanine into Tti2$_{L187P}$. Consistent with this model an allele of *TTI2* encoding an Ala in place of the wild-type Leu (*tti2$_{L187A}$*) grows at near wild-type levels under stress conditions (Figure 2B).

We performed *in vitro* aminoacylation assays to determine the amino acid accepting activity of tRNA$^{Pro}_{UGG}$, tRNA$^{Pro}_{UGG}$ (G3:U70) and tRNA$^{Ala}_{AGC}$ with purified yeast AlaRS and ProRS. AlaRS charges both tRNA$^{Ala}_{AGC}$ and mutant tRNA$^{Pro}_{UGG}$ (G3:U70) with alanine (Figure 3A and Supplementary Figure S2A). Aminoacylation of tRNA$^{Pro}_{UGG}$ with alanine by AlaRS was not detected (Supplementary Figure S2A). Ala-tRNA$^{Ala}_{AGC}$ formation proceeds at an initial rate of 144 ± 15 pmol/min per pmol of AlaRS as compared to 0.6 ± 0.01 pmol/min for Ala-tRNA$^{Pro}_{UGG}$ (G3:U70), an approximate 230-fold decrease in apparent catalytic rate. As expected tRNA$^{Pro}_{UGG}$ was aminoacylated with proline using ProRS (Figure 3B and Supplementary Figure S2B), however, we did not detect the formation of Pro-tRNA$^{Pro}_{UGG}$ (G3:U70) with ProRS (Supplementary Figure S2B). ProRS showed overall less activity compared to AlaRS, with tRNA$^{Pro}_{UGG}$ being aminoacylated at an initial rate of 12 ± 2 fmol/min per pmol of ProRS. Though it is difficult to compare reactions using the different enzymes, AlaRS produced Ala-tRNA$^{Pro}_{UGG}$ (G3:U70) with a greater than 50-fold increase in specific activity compared to cognate Pro-tRNA$^{Pro}_{UGG}$ production by ProRS. Together the *in vitro* experiments show that mutant tRNA$^{Pro}_{UGG}$ (G3:U70) is aminoacylated with alanine but not proline. This provides a mechanistic basis for CCA mistranslation as Ala and indicates that production of the mis-translating Ala-tRNA$^{Pro}_{UGG}$ (G3:U70) species in the cell is at a level such that Ala-tRNA^{Pro} competes with Pro-tRNA^{Pro} for insertion at CCA codons.

To test if suppression affected Tti2$_{L187P}$ expression, we analyzed the steady state level of Tti2$_{L187P}$ with or without *SUF9$_{G3:U70}$* (Supplementary Figure S3). Tti2$_{L187P}$ was elevated 1.1-fold in CY7108 (*SUF9$_{G3:U70}$*) as compared to the CY7020 strain (*SUF9*). Though slight this increase is consistent with an alanine for proline substitution stabilizing the mistranslated protein. To confirm if alanine was in fact incorporated into Tti2$_{L187P}$ *in vivo*, we purified TAP-tagged Tti2$_{L187P}$ from yeast expressing *SUF9$_{G3:U70}$*. The purified proteins were digested with trypsin and peptides containing alanine substitutions identified by electrospray mass spectrometry. Tti2 peptides were detected containing proline or

Downloaded from https://academic.oup.com/nar/article/45/6/3407/2572057 by guest on 21 August 2022

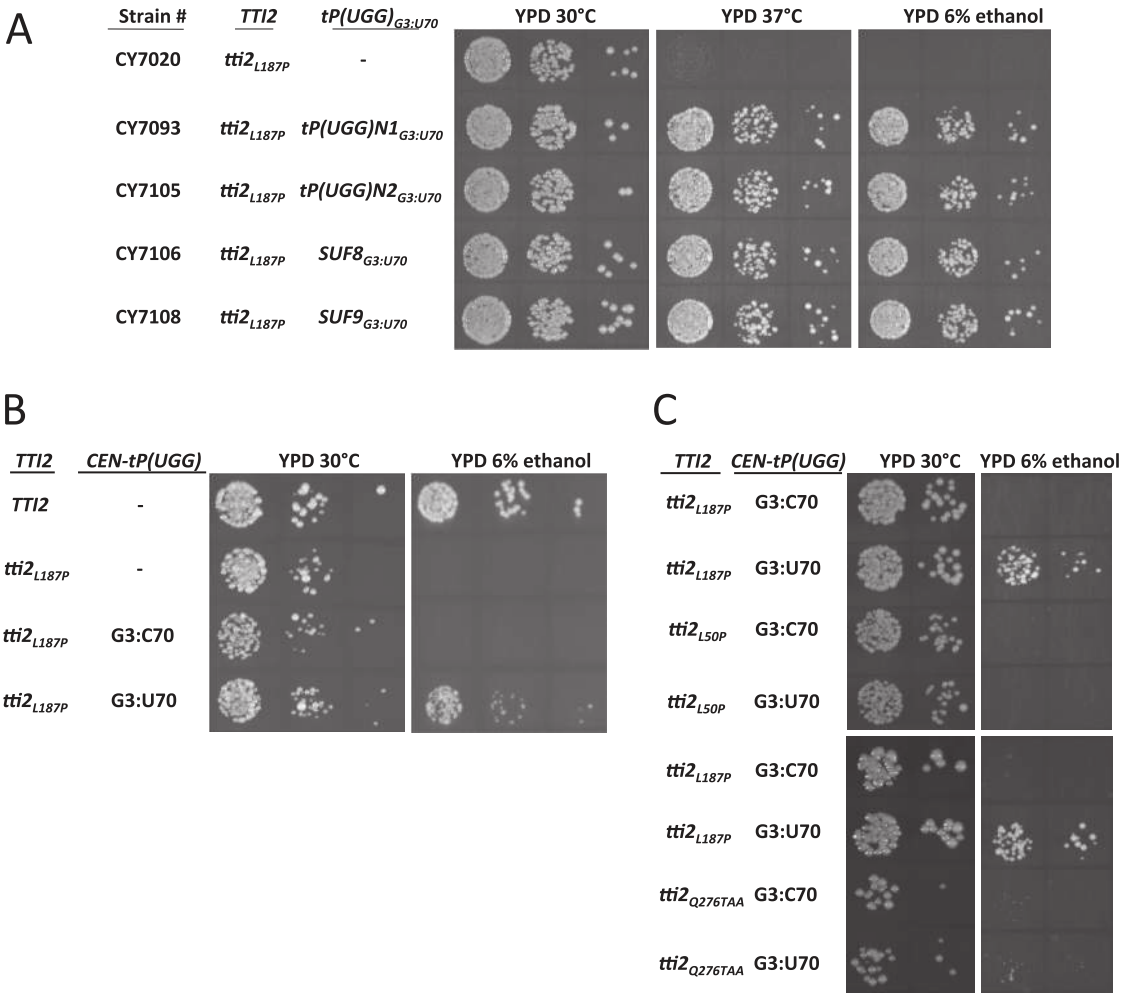

Figure 1. Suppression of $tti2_{L187P}$ by $tRNA^{Pro}_{UGG}$ (G3:U70) alleles. (**A**) Yeast strains CY7020 ($tti2_{L187P}$), CY7093 ($tti2_{L187P}$ $tP(UGG)N1_{G3:U70}$), CY7105 ($tti2_{L187P}$ $tP(UGG)N2_{G3:U70}$), CY7106 ($tti2_{L187P}$ $SUF8_{G3:U70}$), CY7108 ($tti2_{L187P}$ $SUF9_{G3:U70}$) were grown to stationary phase in YPD media. Cell densities were normalized then spotted in 10-fold serial dilutions onto YPD plates and grown at either 30°C or 37°C and onto a YPD plate containing 6% ethanol and grown at 30°C. (**B**) Strain CY6963 containing YCplac33-*DED1-TTI2* (*TTI2*), and CY7020 ($tti2_{L187P}$) containing either YCplac33 (-), YCplac33-*SUF9* (G3:C70) or YCplac33-$SUF9_{G3:U70}$ (G3:U70) were grown to stationary phase in medium lacking uracil, then spotted in 10-fold serial dilutions onto a YPD plate and a YPD plate containing 6% ethanol and grown at 30°C. (**C**) Strains CY7020 ($tti2_{L187P}$), CY6944 ($tti2_{L50P}$) and CY6874 ($tti2_{Q276TAA}$), each containing either YCplac33-*SUF9* (G3:C70) or YCplac33-$SUF9_{G3:U70}$ (G3:U70), were grown to stationary phase in medium lacking uracil, then spotted in 10-fold serial dilutions onto a YPD plate and a YPD plate containing 6% ethanol and grown at 30°C.

Table 1. Suppressor $tRNA^{Pro}$ mutations identified by next generation sequencing

$tRNA_{anticodon}$	Chromosome: Position of Mutation	Mutation Type	Reference Nucleotide	Variant Nucleotide	Reads with Variant	Total Number of Reads
$tP(UGG)N1_{UGG}$	XIV:547193	SNV	C	T	24	24
$tP(UGG)N2_{UGG}$	XIV:568214	SNV	C	T	68	69
$SUF8_{UGG}$	VIII:388896	SNV	C	T	43	43
$SUF9_{UGG}$	VI:101475	SNV	C	T	67	67

alanine at residue 187 (Table 2). A proline to alanine substitution was also detected at Pro245 (CCA codon) in Tti2 peptide V242-K252. Interestingly, two alanine substitutions were detected at CCT codons at Pro280 and Pro327 (Table 2). For each peptide containing amino acid substitutions the wild-type peptide was also detected, indicating ambiguous decoding for each Pro codon.

To estimate the frequency of alanine incorporation at Pro codons by $tRNA^{Pro}_{UGG}$ (G3:U70), we engineered an eGFP reporter protein where mistranslation could be visualized. eGFP was constructed with an Asp to Pro mutation at residue 129 ($eGFP_{D129P}$), a position where proline, but not alanine, disrupts the beta-barrel structure of GFP and eliminates fluorescence. Comparisons were made to a functional $eGFP_{D129A}$ molecule. To localize the GFP sig-

Downloaded from https://academic.oup.com/nar/article/45/6/3407/2572057 by guest on 21 August 2022

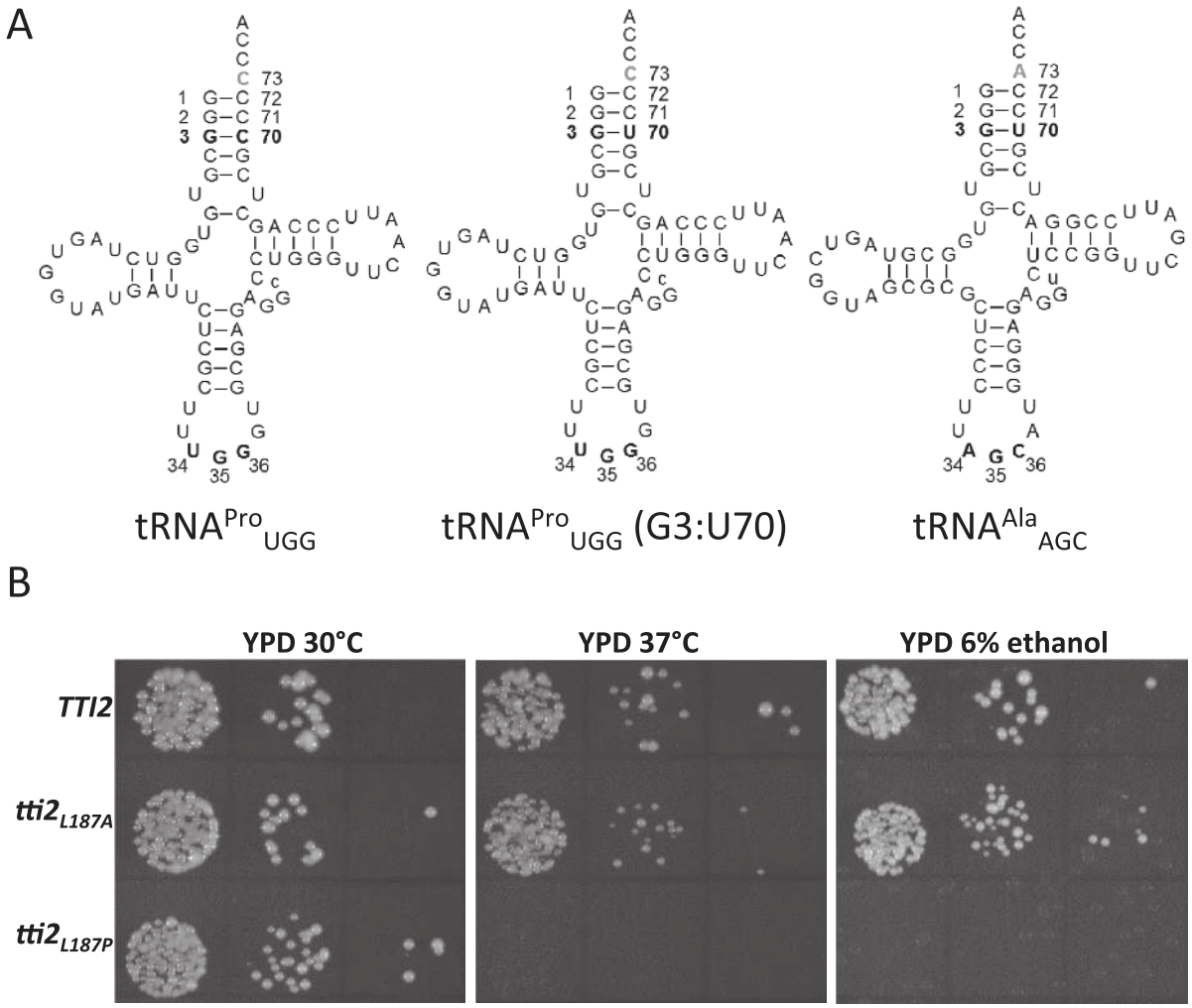

Figure 2. tRNA secondary structures and stress resistance of *tti2*$_{L187A}$. (**A**) Secondary structures of tRNA$^{Pro}_{UGG}$, tRNA$^{Pro}_{UGG}$ (G3:U70) and tRNA$^{Ala}_{AGC}$. Each anticodon and the suppressor mutation position are in bold font. (**B**) Yeast strains CY6857 containing YCplac111-*DED1-TTI2* (*TTI2*), CY7369 containing YCplac111-*DED1-tti2*$_{L187A}$(*tti2*$_{L187A}$) and CY7020 containing YCplac111-*DED1-tti2*$_{L187P}$ (*tti2*$_{L187P}$) were grown to stationary phase in YPD medium. Cell densities were normalized before spotting in 10-fold serial dilutions onto YPD plates and grown at either 30°C or 37°C and onto a YPD plate containing 6% ethanol and grown at 30°C.

Table 2. Alanine substitutions at Pro codons detected by mass spectrometry

Mutated or wild type (wt) residue	Peptide	Sequence Range	Mistranslated Codon	Score¶	Mass (Da)	# Spectrum
P187A*	GVLLAQTLLNHTFM*NETNDSK	183–203	CCA	35.62	2361.163	2
L187P	GVLLPQTLLNHTFMNETNDSK	183–203		47.4	2371.184	7
L187P*	GVLLPQTLLNHTFM*NETNDSK	183–203		32.76	2387.179	3
P245A	VVFATIQSLYK	242–252	CCA	47.48	1267.718	7
P245 (wt)	VVFPTIQSLYK	242–252		48.06	1293.733	315
P280A*	FM*SEIILQNIIAR	269–281	CCT	25.14	1562.849	4
P280 (wt)	FMSEIILQNIIPR	269–281		57.35	1572.87	15
P280 (wt)*	FM*SEIILQNIIPR	269–281		60.24	1588.865	54
P327A	NAFYTTFPK	326–334	CCT	35.16	1087.534	7
P327 (wt)	NPFYTTFPK	326–334		46.72	1113.549	45

*peptides with oxidized methionine resulting in an added mass of 15.99 Daltons.
¶score value was calculated as the negative log base 10 of the *P*-value of the matched peptide. Peptides were considered significant if the false discovery rate of the peptide-spectrum match was less than 1% and the peptide score value was >15.5.
_underlined amino acids represent the position mistranslated or mutated.

Downloaded from https://academic.oup.com/nar/article/45/6/3407/2572057 by guest on 21 August 2022

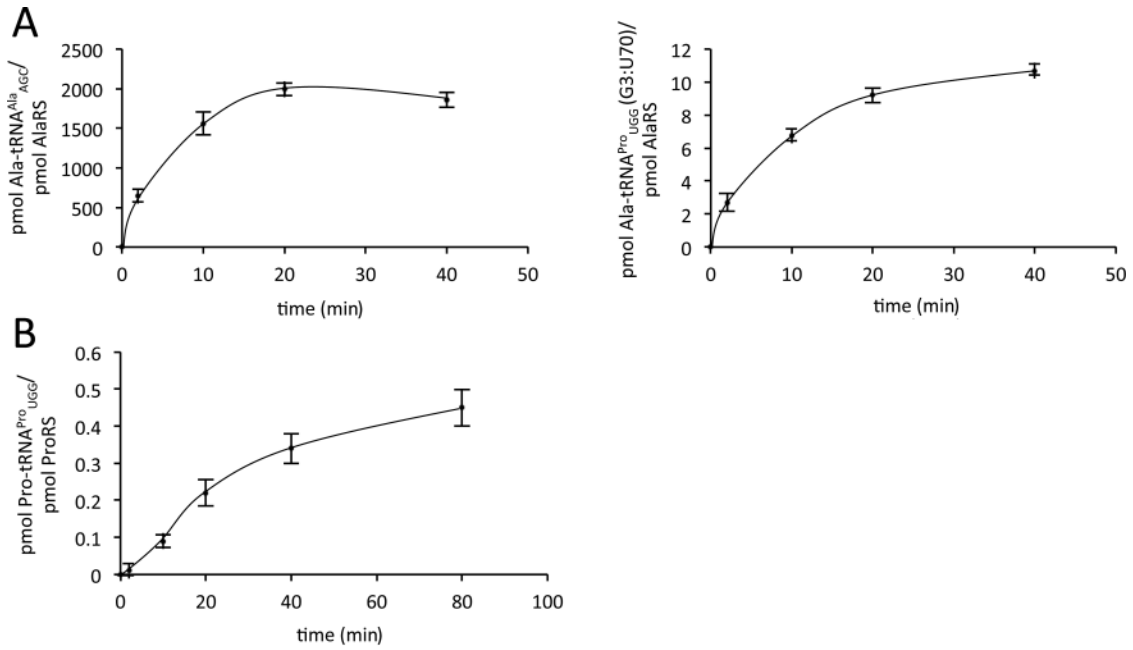

Figure 3. tRNA aminoacylation assays. (**A**) Measurements of alanine aminoacylated $tRNA^{Ala}_{AGC}$ and $tRNA^{Pro}_{UGG}$ (G3:U70) by AlaRS at 0, 2, 10, 20 and 40-min time points. Each measurement represents an average across three technical replicates and the error bars indicate one standard deviation. (**B**) Proline aminoacylation measurements of $tRNA^{Pro}_{UGG}$ at 0, 2, 10, 20, 40 and 80-min time points. Measurements represent an average across three technical replicates with one standard deviation indicated by the error bar.

nal intensity to the nucleus we fused each GFP molecule to Spt7 (45). The nucleus was identified with RFP-tagged Sik1 (32). $eGFP_{D129P}$-Spt7 or $eGFP_{D129A}$-Spt7 were expressed in strains containing either *SUF9* or $SUF9_{G3:U70}$. Fluorescence of $eGFP_{D129P}$ is enhanced in the presence of $SUF9_{G3:U70}$ but not wild-type *SUF9* (Figure 4, Supplementary Figures S1 and S4). Calculating the signal across 150 cells from each strain, we estimate a ∼ 4-fold increase ($P = 0.008$) in the average $eGFP_{D129P}$ fluorescence in the $SUF9_{G3:U70}$ strain compared to the *SUF9* strain (Supplementary Figure S4). To approximate the frequency of alanine incorporation, we compared the signals of $eGFP_{D129P}$ with $eGFP_{D129A}$. In the $SUF9_{G3:U70}$ strain, $eGFP_{D129P}$ signal intensity averaged 8.9% of the $eGFP_{D129A}$ signal, whereas it was 2.8% in the wild-type *SUF9* strain. The difference of these percentages suggests that mistranslation of proline CCA codons by $tRNA^{Pro}_{UGG}$ (G3:U70) occurs at a frequency of ∼6%. Expression of intact $eGFP_{D129P}$-Spt7 was confirmed by Western blot (Supplementary Figure S5), and consistent to what was observed with $Tti2_{L187P}$, $SUF9_{G3:U70}$ slightly increased the level of $eGFP_{D129P}$-Spt7 (1.4-fold).

Suppression of $tti2_{L50P}$ by $SUF2_{G3:U70}$

$tti2_{L50P}$ contains a non-synonymous mutation that alters a CUC to a CCC codon and results in slow growth under stress conditions. *SUF2* encodes $tRNA^{Pro}_{AGG}$, which decodes the CCC codon (46). To examine if the mutant G3:U70 base pair would alter the specificity of a second tRNA, we incorporated the appropriate cytosine to thymine point mutation (Figure 5A) into a plasmid copy of *SUF2* and accessed whether it could suppress $tti2_{L50P}$. $SUF2_{G3:U70}$ suppresses the stress sensitivity caused by $tti2_{L50P}$ in media containing 6% ethanol (Figure 5B). This result suggests that $tRNA^{Pro}_{AGG}$ molecules containing the G3:U70 pair can also be mischarged, likely with alanine, at an efficiency sufficient for suppression of $tti2_{L50P}$.

Impact of introns in $tRNA^{Pro}$ (G3:U70) genes on suppression of *tti2* alleles

Many of the yeast tRNAs including all of the nuclear encoded *tP(UGG)* alleles contain introns. Having a screen in which plasmid encoded $tP(UGG)_{G3:U70}$ is required for growth provided a mechanism to evaluate the role of the intron in *SUF9*. We engineered a mischarging *SUF9* allele lacking the intron (Supplementary Figure S6). The intronless G3:U70 allele, an intron containing G3:U70 allele and the wild-type *SUF9* allele encoded on centromeric plasmids were transformed into CY7020 ($tti2_{L187P}$). The transformed strains were then analyzed for growth on plates containing ethanol. The intronless and intron containing G3:U70 alleles similarly suppressed $tti2_{L187P}$ (Figure 6A).

We also performed the inverse experiment, inserting an intron into the otherwise intronless $SUF2_{G3:U70}$ allele (Supplementary Figure S6). The intron-containing $SUF2_{G3:U70}$ had a slightly reduced ability to suppress slow growth caused by $tti2_{L50P}$ (Figure 6B). This result suggests that the intron in *tP(UGG)* genes partially reduces tRNA maturation or activity.

Cellular response to mistranslation

There are 10 copies of $tRNA^{Pro}_{UGG}$ annotated in S288c derivatives of *S. cerevisiae* (47). As $tRNA^{Pro}_{UGG}$ (G3:U70)

Downloaded from https://academic.oup.com/nar/article/45/6/3407/2572057 by guest on 21 August 2022

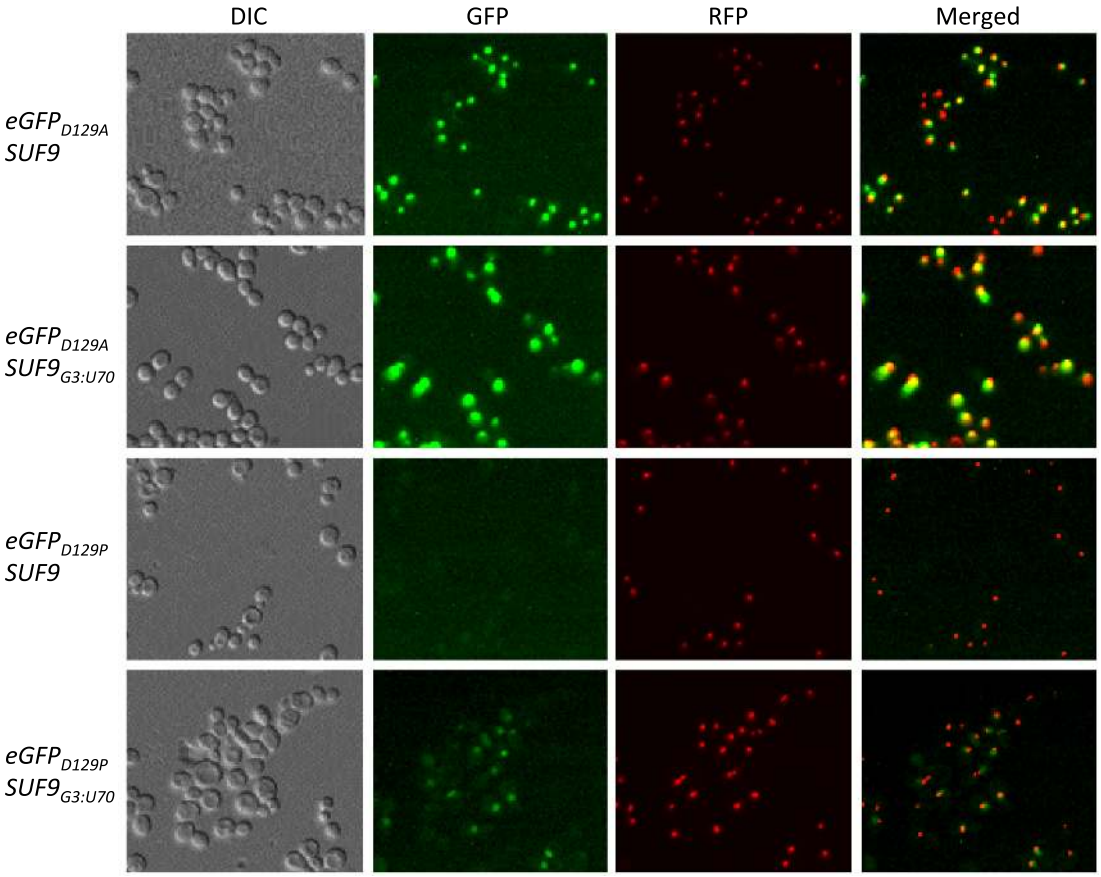

Figure 4. GFP reporter links fluorescence to mistranslation. A yeast strain containing Sik1-RFP was transformed with either YCplac111-*SUF9* (*SUF9*) or YCplac111-*SUF9*$_{G3:U70}$(*SUF9*$_{G3:U70}$), and either YCplac33-*eGFP*$_{D129P}$-*SPT7* (*eGFP*$_{D129P}$) or YCplac33-*eGFP*$_{D129A}$-*SPT7* (*eGFP*$_{D129A}$). Transformants were grown to stationary phase in medium lacking uracil and leucine, diluted 1:20 and grown for 5 h before harvesting cells for imaging. Exposure time for GFP and RFP images was 1 s and the gain was kept constant. Contrast was adjusted uniformly across all GFP images shown.

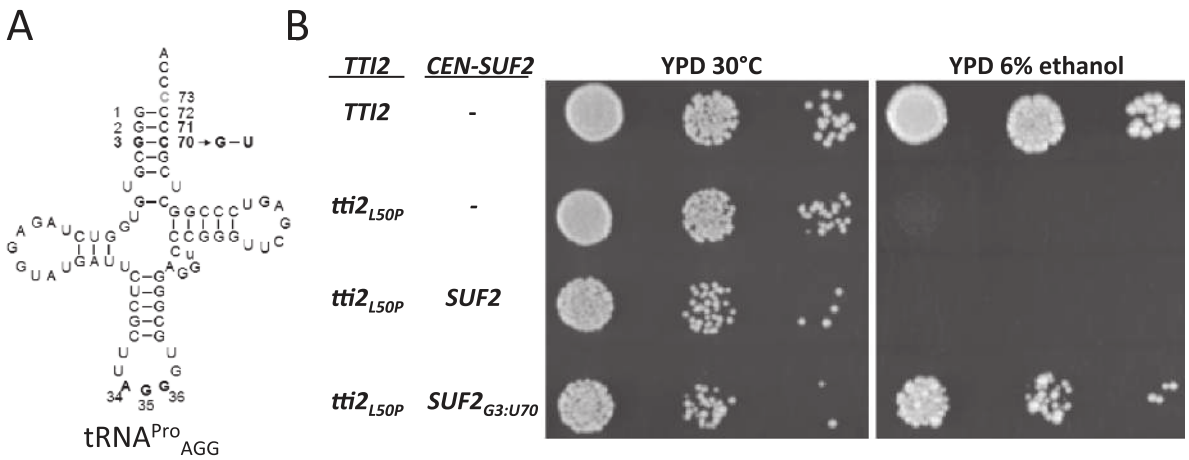

Figure 5. Suppression of *tti2*$_{L50P}$ by *SUF2*$_{G3:U70}$. (**A**) Secondary structure of tRNA$^{Pro}_{AGG}$ showing the suppressor tRNA base pair change (G3:U70) and anticodon in bold font. (**B**) Yeast strains CY6963 (*TTI2*), and CY6944 (*tti2*$_{L50P}$) containing either YCplac33 (-), YCplac33-*SUF2* (*SUF2*) or YCplac33-*SUF2*$_{G3:U70}$ (*SUF2*$_{G3:U70}$) were grown to stationary phase in medium lacking uracil. Cell densities were normalized and cells spotted in 10-fold serial dilutions onto a YPD plate or on a YPD plate containing 6% ethanol and grown at 30°C.

Downloaded from https://academic.oup.com/nar/article/45/6/3407/2572057 by guest on 21 August 2022

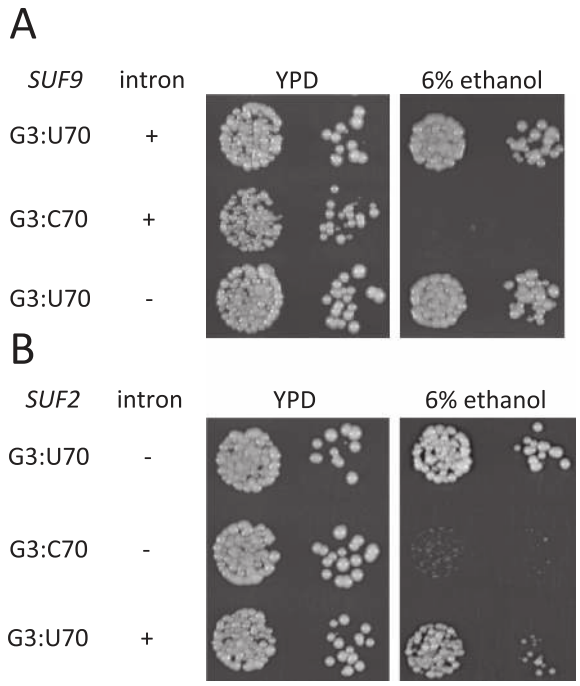

Figure 6. Suppression of *tti2* alleles by intron-containing (+) and intronless (−) tP(UGG) and tP(AGG) alleles. (**A**) CY7020 ($tti2_{L187P}$) containing either YCplac33-*SUF9* (G3:C70), YCplac33-$SUF9_{G3:U70}$ (G3:U70) or YCplac33-$SUF9_{G3:U70}$ (G3:U70) lacking (−) the intron sequence (Δ37–67), were grown to stationary phase in medium lacking uracil, cell densities were normalized and spotted in 10-fold serial dilutions onto a YPD plate and a YPD plate containing 6% ethanol. (**B**) Yeast strain CY6944 ($tti2_{L50P}$) containing either YCplac33-*SUF2* (G3:C70), YCplac33-$SUF2_{G3:U70}$(G3:U70) or YCplac33-$SUF2_{G3:U70}$ with the intron (G3:U70 +) was grown and plated as described above onto a YPD plate and a YPD plate containing 6% ethanol.

results in the mis-incorporation of alanine for proline, we examined the effect of increasing the copy number of this tRNA on cell growth. Strains were constructed that contained $SUF9_{G3:U70}$ (CY7288), $tP(UGG)N1_{G3:U70}$ (CY7355) or both $tP(UGG)N1_{G3:U70}$ and $SUF9_{G3:U70}$ (CY7286) in a background containing wild-type *TTI2*. A single copy of $tP(UGG)_{G3:U70}$, either $tP(UGG)N1_{G3:U70}$ or $SUF9_{G3:U70}$, results in minimal change in growth at 30°C in rich medium or in medium containing 6% ethanol. A reduction in growth was observed for cells grown in 6 μM tunicamycin or under heat stress at 37°C (Figure 7). The presence of two copies of the mis-translating tRNA ($tP(UGG)N1_{G3:U70}$ and $SUF9_{G3:U70}$) slightly reduced growth at 30°C, and exacerbated the growth defect in the stress conditions (Figure 7). In liquid culture, the doubling time during exponential growth increased relative to the wild-type strain by 6 ± 2% and 15 ± 3% in single copy ($SUF9_{G3:U70}$) and double copy ($tP(UGG)N1_{G3:U70}$ $SUF9_{G3:U70}$) strains, respectively (growth curves shown in Supplementary Figure S7). These relatively minor effects on cell growth suggest that the cells have compensation mechanisms to cope with some level of mis-incorporation of alanine at Pro codons (48,49).

We further analyzed the effect of mistranslation on the cellular response to protein stress. Normally cells compensate for mistranslation through induction of the heat shock response (13), therefore, we compared the fluorescent signal intensity resulting from expression of eGFP fused to a heat shock element in strains containing *SUF9* or $SUF9_{G3:U70}$. A wild-type strain grown at 30°C then shifted to 42°C for 1 h shows a 5.8-fold increase in eGFP signal intensity after heat shock (Figure 8A). When comparing strains containing *SUF9* or $SUF9_{G3:U70}$ grown at 30°C, we detected a 3.4-fold increase in eGFP signal intensity caused by $SUF9_{G3:U70}$ (Figure 8A). This result suggests that cells compensate for low levels of mistranslation by partially inducing the heat shock response.

We investigated synthetic interactions between $SUF9_{G3:U70}$ and deletions of genes involved in autophagy (*ATG8*), the unfolded protein response (*IRE1*) or proteasome regulation (*RPN4*). $SUF9_{G3:U70}$ was expressed from a *URA3* centromeric plasmid that was transformed into each deletion strain (*atg8Δ0, ire1Δ0, rpn4Δ0)* and the wild-type yeast strain BY4741. Transformants were spotted on agar plates lacking uracil (Figure 8B). Expression of $SUF9_{G3:U70}$ in the *atg8Δ0* and *ire1Δ0* modestly reduced growth, at a level similar to the wild-type strain. Synthetic slow growth was observed upon expressing the mis-translating tRNA in the *rpn4Δ0* strain. This observation suggests a role for the proteasome in managing cellular stress caused by mistranslation.

We next tested if mistranslation caused by $tRNA^{Pro}_{UGG}$ (G3:U70) might induce protein quality control pathways that could alleviate or exacerbate the growth defects associated with a disease causing allele. The human huntingtin gene contains extensive CAG repeats encoding a toxic polyglutamine tract protein that causes an autosomal-dominant neurodegenerative disorder, known as Huntington's disease (50). We analyzed the consequence of $SUF9_{G3:U70}$ expression in yeast cells containing human huntingtin exon 1 with a 103 residue polyQ tract (*htt103Q*). The *htt103Q* exon was expressed from a galactose inducible promoter on a centromeric plasmid. Wild-type *SUF9* or $SUF9_{G3:U70}$ was expressed from a centromeric plasmid in these strains. Induction of *htt103Q* in galactose-containing medium reduced cell growth (Supplementary Figure S8). Expression of $SUF9_{G3:U70}$ did not change the toxicity resulting from expression of htt103Q. The tRNA-induced mistranslation was unable to rescue the growth defect, but did not further inhibit growth. The data suggest that mistranslation caused by $SUF9_{G3:U70}$ is tolerated in strains containing toxic protein aggregates.

DISCUSSION

The $tti2_{L187P}$ allele provided an efficient system to select for mistranslation and to identify suppressor tRNA mutations. The L187P mutation has a profound effect on cell growth in stress conditions (26). The structure of Tti2 is unknown, but L187 is situated in a predicted alpha helix, which is likely disrupted by the Pro mutation. In addition, a low level of Tti2 is sufficient to support viability (26). We surmise that the low level of Tti2 required to support normal growth is related to the ability of the L187P to select for mistranslation in yeast. The amount of mistranslation required to restore Tti2 function can thus be at a level that is low enough to not compromise viability yet high enough to provide a

Downloaded from https://academic.oup.com/nar/article/45/6/3407/2572057 by guest on 21 August 2022

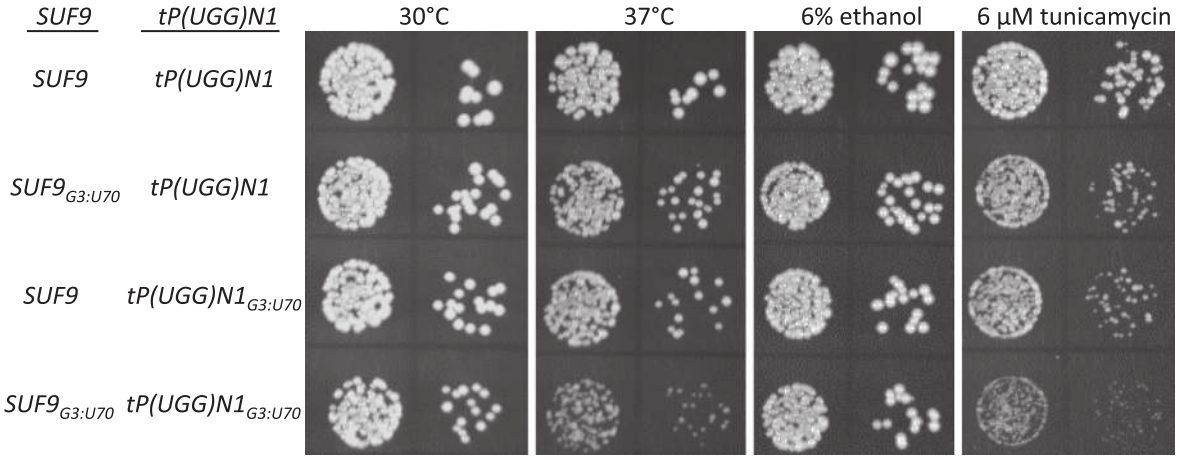

Figure 7. Growth of suppressor tRNA strains under conditions of stress. CY7287 (*SUF9 tP(UGG)N1*), CY7288 (*SUF9*$_{G3:U70}$ *tP(UGG)N1*), CY7355 (*SUF9 tP(UGG)N1*$_{G3:U70}$) and CY7286 (*SUF9*$_{G3:U70}$ *tP(UGG)N1*$_{G3:U70}$) were grown to stationary phase in YPD medium. After normalizing for cell densities cells were spotted in 10-fold serial dilutions onto YPD plates and grown at either 30°C or 37°C, and onto YPD plates containing either 6% ethanol or 6 μM tunicamycin and grown at 30°C.

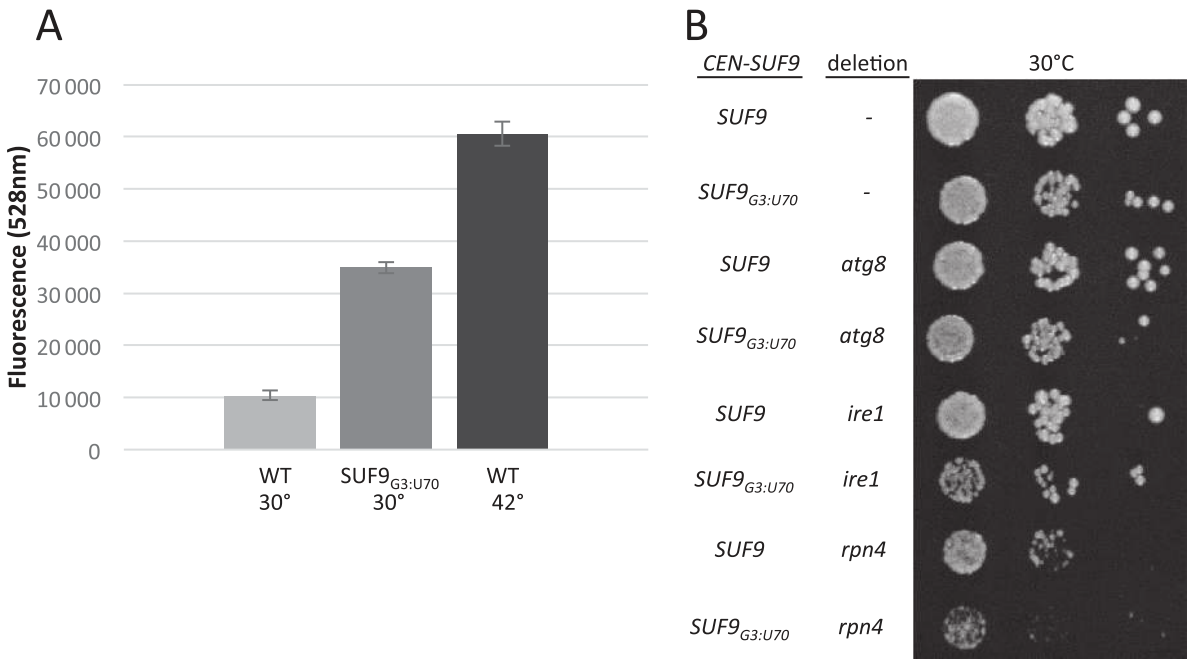

Figure 8. Affects of mistranslation on the heat shock response and proteostasis. (**A**) Yeast strain BY4742 containing *HSE-eGFP* and *SUF9* or *HSE-eGFP* and *SUF9*$_{G3:U70}$ were grown to stationary phase in medium lacking leucine and uracil, diluted 1:100 and grown for 6 h at 30°C. Cell densities were normalized and fluorescence was measured at an emission wavelength of 528 nm. BY4742 containing *HSE-eGFP* and *SUF9* was heat shocked for 1 h at 42°C, cell densities were normalized to the cell densities measured from 30°C growth, and fluorescence was measured at an emission wavelength of 528 nm. A BY4742 strain lacking *HSE-eGFP*, and containing either *SUF9* or *SUF9*$_{G3:U70}$, was used to subtract background fluorescence from each respective experimental strain. All calculations were done using three biological replicates and three technical replicates for each strain. Error bars indicate one standard deviation. (**B**) Yeast strains BY4741 (−), CY1217 (*ire1*), CY2423 (*rpn4*) and CY7450 (*atg8*) expressing either YCplac33-*SUF9* (*SUF9*) or YCplac33-*SUF9*$_{G3:U70}$ (*SUF9*$_{G3:U70}$) were grown to stationary phase in medium lacking uracil. Cell densities were normalized and cells spotted in 10-fold serial dilutions onto a minimal medium plate lacking uracil and grown at 30°C.

sufficient amount of Tti2 for normal growth under stress conditions.

A single nucleotide mutation disrupts the genetic code

The anticipated high fidelity of protein synthesis and the interpretation of the genetic code itself can be disrupted by a single nucleotide mutation. Our genetic screen for suppressors of *tti2*$_{L187P}$ identified four alleles of tP(UGG) with a mutation converting C70U that restored growth in stress conditions. This point mutation changes a G3:C70 base pair in the acceptor stem of tRNA$^{Pro}_{UGG}$ to a G3:U70 base pair. We hypothesized that tRNA$^{Pro}_{UGG}$ (G3:U70) is charged with alanine based on several previous findings. Introducing a single G:U pair in the acceptor stem can be the sole

Downloaded from https://academic.oup.com/nar/article/45/6/3407/2572057 by guest on 21 August 2022

determinant for charging a tRNA molecule with alanine in *E. coli* (44,51). Missense suppressors containing C70U in $tRNA^{Lys}$ have been identified in *E. coli* (24), and are likely charged with either glycine or alanine (52). Finally, the introduction of G3:U70 into a mini RNA helix derived from $tRNA^{Tyr}$ permits charging with alanine (53).

Crystal structures (54) revealed that AlaRS interacts with the minor and major grooves of the acceptor stem of $tRNA^{Ala}$ such that the G3:U70 identity element is required for orientation of the 3′-CCA into the active site of AlaRS. Similarity in the acceptor stems of $tRNA^{Ala}$ and $tRNA^{Pro}$ (Figure 2A), and the extensive interactions between acceptor stem nucleotides and residues of the AlaRS tRNA recognition domain, are plausible reasons for why $tRNA^{Pro}$ containing the G3:U70 pair acts as an efficient substrate for aminoacylation by AlaRS (54).

We have shown that single spontaneous mutations can give rise to tRNA molecules with switched identity, mischarging alanine for proline. Similar results in *E. coli* (44) have led to the idea of that tRNA identity elements are part of a 'second genetic code' that is non-degenerate and more deterministic than the classic view of the code based on accurate pairing of codon and anti-codon (55). Moreover, genetic diversity found in tRNA genes and the discovery of codon reassignments that can be of selective advantage is consistent with an evolving genetic code, contrary to Crick's 'frozen accident' hypothesis (56–60). In *Candida albicans,* serine is incorporated into 97% of Leu CUG codons, suggesting a naturally evolved CUG codon reassignment from Leu to Ser (61). Alterations to the standard genetic code are also found in yeast mitochondrial organelles, bacteria, archaea and viruses (62,63). These findings, along with the identification of pyrrolysine and selenocysteine as natural expansions of the genetic code, suggest that the genetic code continues to evolve (64–66).

Life with mistranslation

A priori, ambiguous decoding or mistranslation should be harmful to the cell due to effects on proteome stability. We examined cells expressing suppressor $tRNA^{Pro}_{UGG}$ (G3:U70) to determine how mistranslation of Pro codons with alanine affects growth and response to protein stress. We found only mild reductions in the growth rates of yeast expressing one or two copies of the mistranslating $tRNA^{Pro}_{UGG}$ (G3:U70) alleles, and a partial induction of the heat shock response caused by $SUF9_{G3:U70}$ expression. These results suggest that yeast tolerate a significant amount of proline to alanine mis-incorporations. This is likely because cells have a number of ways to reduce the toxicity of mis-folded proteins, including the ubiquitin–proteasome system, autophagy, induction of the heat shock response and upregulation of molecular chaperones, and organization of aggregates into inclusion bodies (67,68). The synthetic slow growth upon expressing $SUF9_{G3:U70}$ in a strain deleted for the proteasome regulator Rpn4 does suggest that the ubiquitin–proteasome system is compensating for increased mistranslation arising from Ala-$tRNA^{Pro}_{UGG}$ (G3:U70). Yeast cells overburdened by $tRNA^{Ser}_{CAG}$ mistranslation can adapt when grown for over 250 generations (69). Adaptation is mediated through large genome rearrangements that cause accelerated protein synthesis and protein degradation, and increase glucose uptake to meet energy demands (69). As a consequence of such adaptations, the extent of toxic protein aggregates within the cells is reduced. Additional studies will be required to address whether yeast compensate and adapt to Pro mistranslation by $tRNA^{Pro}_{UGG}$ (G3:U70) over multiple generations.

It is difficult to estimate the extent to which Ala-$tRNA^{Pro}_{UGG}$ (G3:U70) is incorporated into proteins, and it is likely that the rate of mis-incorporation may differ at different Pro codons or based on mRNA sequence context. As there are 10 tP(UGG) genes in the genome, the mutant tRNA may represent roughly 10% of the $tRNA^{Pro}_{UGG}$ pool. The relative amounts of charging of the mutant tRNA with alanine as compared to the wild-type with proline is more difficult to estimate because the reactions involve two different aaRSs. Measurements of initial rates actually suggest that $tRNA^{Pro}_{UGG}$ (G3:U70) is charged more efficiently with alanine than wild-type $tRNA^{Pro}_{UGG}$ with proline. *In vivo* comparisons are further complicated by variations in the amino acid pools and stabilities of the products, though the expression of AlaRS and ProRS is similar (70) and editing or deacylation of mis-charged Ala-$tRNA^{Pro}$ is negligible in *S. cerevisiae* (62). Evaluation of the concentration of the final protein products (e.g. $Tti2_{L187A}$) in cells is also complicated by the potential instability of the $Tti2_{L187P}$ protein. Considering this, we estimated the frequency of Ala-$tRNA^{Pro}_{UGG}$ incorporation into proteins using a GFP reporter assay whereby signal intensity of a $eGFP_{D129P}$ mutant is restored by mistranslation of the CCA Pro codon with alanine. We calculated an approximate 6% increase in $eGFP_{D129P}$ signal intensity as a result of $SUF9_{G3:U70}$ expression. This rate of mistranslation agrees with our estimate that ∼10% of the $tRNA^{Pro}_{UGG}$ pool is mischarged with alanine. The ratio of Tti2 peptides containing proline to alanine substitutions form our mass spectrometry data are also consistent with a rate of mistranslation between 5–10%.

Johansson *et al.* (49) found that a strain deleted for all of the $tRNA^{Pro}_{AGG}$ genes is viable and does not show slow growth. This led them to hypothesize that $tRNA^{Pro}_{UGG}$ molecules can decode all Pro codons. Our finding that $SUF9_{G3:U70}$ (tP(UGG)) does not suppress the L50P mutation, a CCC codon, which is suppressed by $SUF2_{G3:U70}$ (tP(AGG)), suggests that Ala-$tRNA^{Pro}_{UGG}$ molecules do not efficiently decode CCC. Consistent with this, in a strain expressing $SUF9_{G3:U70}$ we detected only proline residues at both CCC codons in Tti2 by mass spectrometry, while alanine incorporations at two of the three CCT codons were identified (Table 2). The $tRNA^{Pro}_{UGG}$ species in *S. cerevisiae* contains 5-carbamoylmethyluridine (ncm^5U) as the only modification at U34 (71). Uridine modifications do not have bond angles required for pairing with C in the ribosome A site (72), however, it is predicted that unmodified uridine can base pair with any nucleoside at the wobble position (72). Therefore, it is possible that uridine in the $tRNA^{Pro}_{UGG}$ anticodon undergoes frequent modification and is unable to decode CCC at the level of efficiency required for suppression of $tti2_{L50P}$.

Downloaded from https://academic.oup.com/nar/article/45/6/3407/2572057 by guest on 21 August 2022

Intron splicing in a mistranslating tRNA

Introns are found in the tRNAs of organisms across all kingdoms of life where they play a role in transcriptional regulation, tRNA modification and prevention of viral genome integration (73). In *S. cerevisiae*, 61 of the 295 tRNA genes contain introns. Removing the intron from $SUF9_{G3:U70}$ had no affect on suppression of $tti2_{L187P}$, suggesting that the intron does not play an essential role in tP(UGG) function. Interestingly, introducing an intron into the tP(AGG) allele $SUF2_{G3:U70}$ partially reduced its ability to suppress. These results are consistent with those of Winey *et al*. (74) who found that removing the intron from a frameshift suppressor allele of *SUF8* improved its translation efficiency. In the case of both the intronless *SUF2* and *SUF8,* the increased activity may be due to increased levels of the tRNA by removing the need of a potentially inefficient splicing step (74). In this regard, the intron may play a role in regulating the abundance of mature tRNA.

CONCLUSION

Our study prompts further evaluation of the idea that a 'frozen' genetic code is a prerequisite for life. Rather we demonstrate that mistranslation can arise via a single nucleotide mutation as a route to circumvent lethal mutations in the genome. The tRNAs we have identified are relatively efficient at missense suppression and these tRNAs will continue to be useful tools for genetic analyses and synthetic biology applications (e.g. (75)). The spontaneous nature of the selection process and the limited consequences of the genetic code change on growth suggest that tRNA alleles resulting in mis-aminoacylation may become fixed in a population where they confer advantage and may be more common than previously assumed. Otherwise deleterious mutations in coding regions may become phenotypically neutral due to the cell's ability to reinterpret the meaning of codons leading to ambiguous decoding and mistranslation.

SUPPLEMENTARY DATA

Supplementary Data are available at NAR Online.

ACKNOWLEDGEMENTS

The authors are grateful to Ilka Heinemann, Dieter Söll and Julie Genereaux for critical discussions and suggestions on the manuscript. The authors thank Paula Pittock, David Carter and John Robinson for their expertise and assistance with mass spectrometry and next generation sequencing experiments. The authors also thank Christina Cheung for assistance with tRNA production, Patrick Lajoie for providing the anti-GFP antibody and Martin Duennwald for providing *htt103Q* and *HSE-eGFP* plasmids and the Sik1-RFP yeast strain.

FUNDING

Natural Sciences and Engineering Research Council of Canada [RGPIN-2015-04394 to C.J.B. and RGPIN 04282-2014 to P.O.]; Canada Foundation for Innovation [229917 to P.O.]; Ontario Research Fund [229917 to P.O.]; Canada Research Chairs [950-229917 to P.O.]; Bishnu Sanwal and Theodore Lo Graduate Endowment Fund; M.D.B holds an Alexander Graham Bell Canada Graduate Scholarship (CGSM) in NSERC. Funding for open access charge: NSERC [RGPIN 04282-2014 to P.O.].
Conflict of interest statement. None declared.

REFERENCES

1. Loftfield,R.B. and Vanderjagt,D. (1972) The frequency of errors in protein biosynthesis. *Biochem. J.*, **128**, 1353–1356.
2. Ibba,M. and Söll,D. (2000) Aminoacyl-tRNA synthesis. *Annu. Rev. Biochem.*, **69**, 617–650.
3. Giegé,R., Sissler,M. and Florentz,C. (1998) Universal rules and idiosyncratic features in tRNA identity. *Nucleic Acids Res.*, **26**, 5017–5035.
4. Beuning,P.J. and Musier-Forsyth,K. (1999) Transfer RNA recognition by aminoacyl-tRNA synthetases. *Biopolymers*, **52**, 1–28.
5. Park,S.J., Hou,Y.M. and Schimmel,P. (1989) A single base pair affects binding and catalytic parameters in the molecular recognition of a transfer RNA. *Biochemistry*, **28**, 2740–2746.
6. Ibba,M., Hong,K.W., Sherman,J.M., Sever,S. and Söll,D. (1996) Interactions between tRNA identity nucleotides and their recognition sites in glutaminyl-tRNA synthetase determine the cognate amino acid affinity of the enzyme. *Proc. Natl. Acad. Sci. U.S.A.*, **93**, 6953–6958.
7. Aldinger,C.A., Leisinger,A.K. and Igloi,G.L. (2012) The influence of identity elements on the aminoacylation of tRNA(Arg) by plant and Escherichia coli arginyl-tRNA synthetases. *FEBS J.*, **279**, 3622–3638.
8. Yuan,J., Gogakos,T., Babina,A.M., Söll,D. and Randau,L. (2011) Change of tRNA identity leads to a divergent orthogonal histidyl-tRNA synthetase/tRNAHis pair. *Nucleic Acids Res.*, **39**, 2286–2293.
9. Muramatsu,T., Nishikawa,K., Nemoto,F., Kuchino,Y., Nishimura,S., Miyazawa,T. and Yokoyama,S. (1988) Codon and amino-acid specificities of a transfer-RNA are both converted by a single post-transcriptional modification. *Nature*, **336**, 179–181.
10. Perret,V., Garcia,A., Grosjean,H., Ebel,J.P., Florentz,C. and Giege,R. (1990) Relaxation of a transfer RNA specificity by removal of modified nucleotides. *Nature*, **344**, 787–789.
11. Perona,J.J. and Gruic-Sovulj,I. (2014) Synthetic and editing mechanisms of aminoacyl-tRNA synthetases. *Top Curr. Chem.*, **344**, 1–41.
12. Reynolds,N.M., Lazazzera,B.A. and Ibba,M. (2010) Cellular mechanisms that control mistranslation. *Nat. Rev. Microbiol.*, **8**, 849–856.
13. Ruan,B., Palioura,S., Sabina,J., Marvin-Guy,L., Kochhar,S., Larossa,R.A. and Söll,D. (2008) Quality control despite mistranslation caused by an ambiguous genetic code. *Proc. Natl. Acad. Sci. U.S.A.*, **105**, 16502–16507.
14. Liu,Z., Vargas-Rodriguez,O., Goto,Y., Novoa,E.M., Ribas de Pouplana,L., Suga,H. and Musier-Forsyth,K. (2015) Homologous trans-editing factors with broad tRNA specificity prevent mistranslation caused by serine/threonine misactivation. *Proc. Natl. Acad. Sci. U.S.A.*, **112**, 6027–6032.
15. Schimmel,P. (2008) Development of tRNA synthetases and connection to genetic code and disease. *Protein Sci.*, **17**, 1643–1652.
16. Lee,J.W., Beebe,K., Nangle,L.A., Jang,J., Longo-Guess,C.M., Cook,S.A., Davisson,M.T., Sundberg,J.P., Schimmel,P. and Ackerman,S.L. (2006) Editing-defective tRNA synthetase causes protein misfolding and neurodegeneration. *Nature*, **443**, 50–55.
17. Liu,Y., Satz,J.S., Vo,M.N., Nangle,L.A., Schimmel,P. and Ackerman,S.L. (2014) Deficiencies in tRNA synthetase editing activity cause cardioproteinopathy. *Proc. Natl. Acad. Sci. U.S.A.*, **111**, 17570–17575.
18. Ribas de Pouplana,L, Santos,M.A., Zhu,J.H., Farabaugh,P.J. and Javid,B. (2014) Protein mistranslation: friend or foe? *Trends Biochem. Sci.*, **39**, 355–362.
19. Pezo,V., Metzgar,D., Hendrickson,T.L., Waas,W.F., Hazebrouck,S., Doring,V., Marliere,P., Schimmel,P. and De Crecy-Lagard,V. (2004) Artificially ambiguous genetic code confers growth yield advantage. *Proc. Natl. Acad. Sci. U.S.A.*, **101**, 8593–8597.

Downloaded from https://academic.oup.com/nar/article/45/6/3407/2572057 by guest on 21 August 2022

20. Netzer,N., Goodenbour,J.M., David,A., Dittmar,K.A., Jones,R.B., Schneider,J.R., Boone,D., Eves,E.M., Rosner,M.R., Gibbs,J.S. *et al.* (2009) Innate immune and chemically triggered oxidative stress modifies translational fidelity. *Nature*, **462**, 522–526.
21. Reynolds,N.M., Ling,J., Roy,H., Banerjee,R., Repasky,S.E., Hamel,P. and Ibba,M. (2010) Cell-specific differences in the requirements for translation quality control. *Proc. Natl. Acad. Sci. U.S.A.*, **107**, 4063–4068.
22. Schwartz,M.H. and Pan,T. (2016) Temperature dependent mistranslation in a hyperthermophile adapts proteins to lower temperatures. *Nucleic Acids Res.*, **44**, 294–303.
23. Qian,Q., Li,J.N., Zhao,H., Hagervall,T.G., Farabaugh,P.J. and Bjork,G.R. (1998) A new model for phenotypic suppression of frameshift mutations by mutant tRNAs. *Mol. Cell*, **1**, 471–482.
24. Prather,N.E., Murgola,E.J. and Mims,B.H. (1984) Nucleotide substitution in the amino acid acceptor stem of lysine transfer RNA causes missense suppression. *J. Mol. Biol.*, **172**, 177–184.
25. Singaravelan,B., Roshini,B.R. and Munavar,M.H. (2010) Evidence that the supE44 mutation of Escherichia coli is an amber suppressor allele of glnX and that it also suppresses ochre and opal nonsense mutations. *J. Bacteriol.*, **192**, 6039–6044.
26. Hoffman,K.S., Duennwald,M.L., Karagiannis,J., Genereaux,J., McCarton,A.S. and Brandl,C.J. (2016) Saccharomyces cerevisiae Tti2 Regulates PIKK Proteins and Stress Response. *G3 (Bethesda)*, **6**, 1649–1659.
27. Hurov,K.E., Cotta-Ramusino,C. and Elledge,S.J. (2010) A genetic screen identifies the Triple T complex required for DNA damage signaling and ATM and ATR stability. *Genes Dev.*, **24**, 1939–1950.
28. Stirling,P.C., Bloom,M.S., Solanki-Patil,T., Smith,S., Sipahimalani,P., Li,Z., Kofoed,M., Ben-Aroya,S., Myung,K. and Hieter,P. (2011) The complete spectrum of yeast chromosome instability genes identifies candidate CIN cancer genes and functional roles for ASTRA complex components. *PLoS Genet.*, **7**, e1002057.
29. Takai,H., Xie,Y., de Lange,T. and Pavletich,N.P. (2010) Tel2 structure and function in the Hsp90-dependent maturation of mTOR and ATR complexes. *Genes Dev.*, **24**, 2019–2030.
30. Winzeler,E.A. and Davis,R.W. (1997) Functional analysis of the yeast genome. *Curr. Opin. Genet. Dev.*, **7**, 771–776.
31. Gelperin,D.M., White,M.A., Wilkinson,M.L., Kon,Y., Kung,L.A., Wise,K.J., Lopez-Hoyo,N., Jiang,L., Piccirillo,S., Yu,H. *et al.* (2005) Biochemical and genetic analysis of the yeast proteome with a movable ORF collection. *Genes Dev.*, **19**, 2816–2826.
32. Huh,W.K., Falvo,J.V., Gerke,L.C., Carroll,A.S., Howson,R.W., Weissman,J.S. and O'Shea,E.K. (2003) Global analysis of protein localization in budding yeast. *Nature*, **425**, 686–691.
33. Tong,A.H., Evangelista,M., Parsons,A.B., Xu,H., Bader,G.D., Page,N., Robinson,M., Raghibizadeh,S., Hogue,C.W., Bussey,H. *et al.* (2001) Systematic genetic analysis with ordered arrays of yeast deletion mutants. *Science*, **294**, 2364–2368.
34. Hoke,S.M., Liang,G., Mutiu,A.I., Genereaux,J. and Brandl,C.J. (2007) C-terminal processing of yeast Spt7 occurs in the absence of functional SAGA complex. *BMC Biochem.*, **8**, 16.
35. Hoke,S.M., Guzzo,J., Andrews,B. and Brandl,C.J. (2008) Systematic genetic array analysis links the Saccharomyces cerevisiae SAGA/SLIK and NuA4 component Tra1 to multiple cellular processes. *BMC Genet.*, **9**, 46.
36. Duennwald,M.L., Jagadish,S., Muchowski,P.J. and Lindquist,S. (2006) Flanking sequences profoundly alter polyglutamine toxicity in yeast. *Proc. Natl. Acad. Sci. U.S.A.*, **103**, 11045–11050.
37. Oshikane,H., Sheppard,K., Fukai,S., Nakamura,Y., Ishitani,R., Numata,T., Sherrer,R.L., Feng,L., Schmitt,E., Panvert,M. *et al.* (2006) Structural basis of RNA-dependent recruitment of glutamine to the genetic code. *Science*, **312**, 1950–1954.
38. Gregan,J., Riedel,C.G., Petronczki,M., Cipak,L., Rumpf,C., Poser,I., Buchholz,F., Mechtler,K. and Nasmyth,K. (2007) Tandem affinity purification of functional TAP-tagged proteins from human cells. *Nat. Protoc.*, **2**, 1145–1151.
39. O'Donoghue,P., Sheppard,K., Nureki,O. and Soll,D. (2011) Rational design of an evolutionary precursor of glutaminyl-tRNA synthetase. *Proc. Natl. Acad. Sci. U.S.A.*, **108**, 20485–20490.
40. Ginestet,C. (2011) ggplot2: Elegant Graphics for Data Analysis. *J. R. Stat. Soc. A*, **174**, 245–245.
41. Mutiu,A.I., Hoke,S.M., Genereaux,J., Hannam,C., MacKenzie,K., Jobin-Robitaille,O., Guzzo,J., Cote,J., Andrews,B., Haniford,D.B. *et al.* (2007) Structure/function analysis of the phosphatidylinositol-3-kinase domain of yeast tra1. *Genetics*, **177**, 151–166.
42. Imura,N., Weiss,G.B. and Chambers,R.W. (1969) Reconstitution of alanine acceptor activity from fragments of yeast tRNA-Ala II. *Nature*, **222**, 1147–1148.
43. Hou,Y.M. and Schimmel,P. (1989) Evidence that a major determinant for the identity of a transfer RNA is conserved in evolution. *Biochemistry*, **28**, 6800–6804.
44. Hou,Y.M. and Schimmel,P. (1988) A simple structural feature is a major determinant of the identity of a transfer RNA. *Nature*, **333**, 140–145.
45. Gansheroff,L.J., Dollard,C., Tan,P. and Winston,F. (1995) The Saccharomyces cerevisiae SPT7 gene encodes a very acidic protein important for transcription in vivo. *Genetics*, **139**, 523–536.
46. Hani,J. and Feldmann,H. (1998) tRNA genes and retroelements in the yeast genome. *Nucleic Acids Res.*, **26**, 689–696.
47. Chan,P.P. and Lowe,T.M. (2009) GtRNAdb: a database of transfer RNA genes detected in genomic sequence. *Nucleic Acids Res.*, **37**, 93–97.
48. Bonitz,S.G., Berlani,R., Coruzzi,G., Li,M., Macino,G., Nobrega,F.G., Nobrega,M.P., Thalenfeld,B.E. and Tzagoloff,A. (1980) Codon recognition rules in yeast mitochondria. *Proc. Natl. Acad. Sci. U.S.A.*, **77**, 3167–3170.
49. Johansson,M.J., Esberg,A., Huang,B., Bjork,G.R. and Bystrom,A.S. (2008) Eukaryotic wobble uridine modifications promote a functionally redundant decoding system. *Mol. Cell. Biol.*, **28**, 3301–3312.
50. Ross,C.A. and Tabrizi,S.J. (2011) Huntington's disease: from molecular pathogenesis to clinical treatment. *Lancet Neurol.*, **10**, 83–98.
51. McClain,W.H. and Foss,K. (1988) Changing the identity of a tRNA by introducing a G-U wobble pair near the 3' acceptor end. *Science*, **240**, 793–796.
52. Murgola,E.J. and Pagel,F.T. (1983) Suppressors of lysine codons may be misacylated lysine tRNAs. *J. Bacteriol.*, **156**, 917–919.
53. Francklyn,C. and Schimmel,P. (1989) Aminoacylation of RNA minihelices with alanine. *Nature*, **337**, 478–481.
54. Naganuma,M., Sekine,S., Chong,Y.E., Guo,M., Yang,X.L., Gamper,H., Hou,Y.M., Schimmel,P. and Yokoyama,S. (2014) The selective tRNA aminoacylation mechanism based on a single G*U pair. *Nature*, **510**, 507–511.
55. de Duve,C. (1988) Transfer RNAs: the second genetic code. *Nature*, **333**, 117–118.
56. Crick,F.H. (1968) The origin of the genetic code. *J. Mol. Biol.*, **38**, 367–379.
57. Santos,M.A., Cheesman,C., Costa,V., Moradas-Ferreira,P. and Tuite,M.F. (1999) Selective advantages created by codon ambiguity allowed for the evolution of an alternative genetic code in Candida spp. *Mol. Microbiol.*, **31**, 937–947.
58. Santos,M.A., Moura,G., Massey,S.E. and Tuite,M.F. (2004) Driving change: the evolution of alternative genetic codes. *Trends Genet.*, **20**, 95–102.
59. Goodenbour,J.M. and Pan,T. (2006) Diversity of tRNA genes in eukaryotes. *Nucleic Acids Res.*, **34**, 6137–6146.
60. Parisien,M., Wang,X.Y. and Pan,T. (2013) Diversity of human tRNA genes from the 1000-genomes project. *RNA Biol.*, **10**, 1853–1867.
61. Bezerra,A.R., Simoes,J., Lee,W., Rung,J., Weil,T., Gut,I.G., Gut,M., Bayes,M., Rizzetto,L., Cavalieri,D. *et al.* (2013) Reversion of a fungal genetic code alteration links proteome instability with genomic and phenotypic diversification. *Proc. Natl. Acad. Sci. U.S.A.*, **110**, 11079–11084.
62. Ling,J.Q., O'Donoghue,P. and Soll,D. (2015) Genetic code flexibility in microorganisms: novel mechanisms and impact on physiology. *Nat. Rev. Microbiol.*, **13**, 707–721.
63. Ambrogelly,A., Palioura,S. and Soll,D. (2007) Natural expansion of the genetic code. *Nat. Chem. Biol.*, **3**, 29–35.
64. Soll,D. (1988) Genetic-Code - Enter a New Amino-Acid. *Nature*, **331**, 662–663.
65. Hao,B., Gong,W.M., Ferguson,T.K., James,C.M., Krzycki,J.A. and Chan,M.K. (2002) A new UAG-encoded residue in the structure of a methanogen methyltransferase. *Science*, **296**, 1462–1466.

Downloaded from https://academic.oup.com/nar/article/45/6/3407/2572057 by guest on 21 August 2022

66. Srinivasan,G., James,C.M. and Krzycki,J.A. (2002) Pyrrolysine encoded by UAG in Archaea: Charging of a UAG-decoding specialized tRNA. *Science*, **296**, 1459–1462.
67. Chen,B., Retzlaff,M., Roos,T. and Frydman,J. (2011) Cellular strategies of protein quality control. *Cold Spring Harb. Perspect. Biol.*, **3**, a004374.
68. Ciechanover,A. and Kwon,Y.T. (2015) Degradation of misfolded proteins in neurodegenerative diseases: therapeutic targets and strategies. *Exp. Mol. Med.*, **47**, e147.
69. Kalapis,D., Bezerra,A.R., Farkas,Z., Horvath,P., Bodi,Z., Daraba,A., Szamecz,B., Gut,I., Bayes,M., Santos,M.A. *et al.* (2015) Evolution of Robustness to Protein Mistranslation by Accelerated Protein Turnover. *PLoS Biol.*, **13**, e1002291.
70. Kulak,N.A., Pichler,G., Paron,I., Nagaraj,N. and Mann,M. (2014) Minimal, encapsulated proteomic-sample processing applied to copy-number estimation in eukaryotic cells. *Nat. Methods*, **11**, 319–324.
71. Keith,G., Desgres,J., Pochart,P., Heyman,T., Kuo,K.C. and Gehrke,C.W. (1990) Eukaryotic tRNAs(Pro): primary structure of the anticodon loop; presence of 5-carbamoylmethyluridine or inosine as the first nucleoside of the anticodon. *Biochim. Biophys. Acta*, **1049**, 255–260.
72. Lim,V.I. (1994) Analysis of action of wobble nucleoside modifications on codon-anticodon pairing within the ribosome. *J. Mol. Biol.*, **240**, 8–19.
73. Yoshihisa,T. (2014) Handling tRNA introns, archaeal way and eukaryotic way. *Front. Genet.*, **5**, 213.
74. Winey,M., Mendenhall,M.D., Cummins,C.M., Culbertson,M.R. and Knapp,G. (1986) Splicing of a yeast proline tRNA containing a novel suppressor mutation in the anticodon stem. *J. Mol. Biol.*, **192**, 49–63.
75. Brandon,H.E., Friedt,J.R., Glaister,G.D., Kharey,S.K., Smith,D.D., Stinson,Z.K. and Wieden,H.J. (2015) Introducing a class of standardized and interchangeable parts utilizing programmed ribosomal frameshifts for synthetic biology applications. *Translation (Austin)*, **3**, e1112458.

Downloaded from https://academic.oup.com/nar/article/45/6/3407/2572057 by guest on 21 August 2022